

Comparison of CT and adjusted MRI for evaluating paranasal sinuses surgical key landmarks*

Roe Landsberg¹, Shay Schneider¹, Muhamed Masalha¹, Ariel Margulis¹, Michal Guindy², Judith Luckman²

Rhinology Online, Vol 5: 37 - 43, 2022

<http://doi.org/10.4193/RHINOL/21.022>

¹ A.R.M. Center of Otolaryngology/Head and Neck Surgery, Assuta Medical Centers, Tel Aviv, Israel

² Department of Radiology, Assuta Medical Centers, Tel Aviv, Israel

***Received for publication:**

May 18, 2021

Accepted: February 17, 2022

Published: March 28, 2022

Abstract

Background: Sinus CT is the imaging technique of choice for planning endoscopic sinus surgery (ESS). Although MRI has a better soft tissue demonstration, it is not commonly used for ESS due to suboptimal bone demonstration. We hypothesised that adjustment of certain MRI parameters, would allow better demonstration of bones and enable the surgeon to adequately identify surgical landmarks.

Methodology: Twenty patients identified as candidates for ESS underwent CT and adjusted MRI exams of the paranasal sinuses (40 in total). rhinologist and a neuroradiologist independently compared and graded 46 bony structures (23 on each side) in each patient's CT and MRI. Overall, 920 anatomical structures were graded by each observer (1840 structures in total). Statistical analysis included overall and per variable grading distribution for each observer, and overall agreement.

Results: MRI images were equal, or superior to CT for assessing paranasal anatomy in 66.8% and 86.4% of structures evaluated by the rhinologist and neuroradiologist, respectively. Overall agreement between observers (77%) was moderate.

Conclusion: The rhinologist prefers CT demonstration of bony structures, while the neuroradiologist prefers MRI. Still, with the MRI protocol used in this study, according to both, most bony structures are well demonstrated by MRI.

Key words: computed tomography, magnetic resonance imaging, endoscopic sinus surgery, diagnosis, bony structures

Introduction

The paranasal sinus complex is a labyrinth of air-filled cells separated by a thin bony septae. Paranasal sinuses structure varies greatly among patients. Additionally, their structure may differ between the right and left side of the same patient, rendering accurate orientation essential for operative precision. When considering endoscopic sinus surgery (ESS), a sinus computed tomography (CT) scan is indicated for two main reasons: first, the CT scan demonstrates disease presence and its extent, thereby helping the surgeon decide whether surgery is indicated. Second, due to the complex anatomy of the paranasal sinuses and their proximity to vital structures, such as the brain, eyes and carotid artery, the surgeon uses the CT scan intraoperatively as a roadmap for the surgical steps and to prevent severe com-

plications such as blindness, brain damage or massive bleeding. Moreover, the CT scan is considered the imaging of choice since it provides a clear demonstration of the bony septae and hence contributes to precision and safety during surgery.

A unique feature of recent decades is that patients independently obtain information about possible risks from various sources (television, internet, etc.). One of the main drawbacks of CT is the radiation associated with acquiring images. Although CT technology has changed significantly over the years with lower dose exposures noted⁽¹⁾, many patients still fear radiation-emitting devices. For many patients who may be candidates for ESS, the preoperative CT scan is not their first. nor likely to be their last CT exam, hence the fear of developing a neoplastic disease and cataract can lead patients to become overly cauti-

ous during their presurgical assessment⁽²⁻⁶⁾.

Another well-known disadvantage of CT is poor soft tissue demonstration. In contrast to CT, magnetic resonance imaging (MRI) provides excellent soft tissue demonstration and does not involve ionizing radiation^(7,8). However, the disadvantages of MRI include suboptimal demonstration of bony structures, high cost, longer examination time and lower accessibility^(7,8).

To overcome these obstacles, the authors hypothesize that by improving certain MRI parameters a better demonstration of the bony septae of the nose and paranasal sinuses can be achieved to a degree where, at least in certain and highly selected indications, the surgeon would be able to rely on MRI preoperatively and during surgery. If achieved, the surgeon will be able to clearly visualize both hard and soft tissue features while reducing patients' exposure to radiation.

Methods

Patients and setting

This prospective study was reviewed and approved by the local institutional ethics committee. The study was performed during 2019-2020. Patients with chronic rhinosinusitis and without other comorbidities who were candidates for ESS at Assuta Medical Centers were included in the study. Revision cases were excluded.

The patients were referred to a routine CT scan of the paranasal sinuses at the radiology department as part of the routine management. Following the CT scan, the patients signed an informed consent and underwent MRI of the paranasal sinuses.

Imaging protocol

The MRI protocol was developed by experienced neuroradiologist (J.L.), a rhinologist/endoscopic surgeon (R.L.) and an MRI technician to enable a usable demonstration of the nose, septae and bony structures of the paranasal sinuses during endoscopic surgery.

To establish the protocol, the rhinologist selected 23 specific nose and paranasal bony structures to serve as key anatomical landmarks for orientation during surgery. These bony elements included intranasal and paranasal sinus structures, and framework-related bony elements that separate the nose and paranasal sinuses from adjacent vital structures: the brain, orbit and blood vessels (Table 1). Next, the neuroradiologist and the rhinologist evaluated various MRI sequences by comparing pairs of CT and MRI scans of four patients until the optimal protocol was agreed upon.

The following MRI protocol was employed: volumetric sequences, unenhanced, T1 and T2 sagittal turbo spin echo (TSE) 0.9-mm sections with three-dimensional (3D) reconstruction, for axial and coronal planes, and direct coronal 0.9-1-mm sections T1 and T2 3D TSE images (Magnetom Aera 1.5 Tesla, Siemens Healthcare).

Table 1. Observed bony elements in the nose and paranasal sinuses.

Nose	Septum, inferior turbinates, middle turbinates, superior turbinates
Sinuses outer contour	Frontal, maxillary, anterior ethmoid, posterior ethmoid, sphenoid
Sinuses inner septae	Frontal, ethmoid, sphenoid
Specific bony structures	Agger nasi, uncinat process, bulla, lamina papyracea, anterior ethmoid artery canal, posterior ethmoid artery canal, infra orbital nerve canal
Skull base structures	Cribriform plate, sella turcica, optic nerve canal, carotid artery canal, vidian nerve canal, rotundum nerve canal.

Image analysis

Following optimization of the MRI protocols, the rhinologist and the neuroradiologist observed and evaluated the CT and MRI images of each of the study participants independently. Each structure was first identified on the CT scan, which served as the reference image. Then, the same structure was located on the MRI image and graded on a scale of 1 to 4 as follows: 1) not visible at all on MRI, 2) demonstrated less than in CT (CT superior), 3) demonstrated the same as in CT, 4) demonstrated better than in CT (MRI superior). Overall, 920 anatomical structures were graded by each observer.

Statistical analysis

The grades provided by the rhinologist and neuroradiologist for the comparison of pairs of CT and MRI images were summarised using absolute frequency, relative frequency, and confidence intervals for proportion by specialty (rhinologist/neuroradiologist) and by anatomical structures. Confidence intervals for the proportion of "MRI same or superior" (i.e., pooled grades 3 and 4) were also computed. The strength of agreement between the rhinologist and the neuroradiologist was calculated using Kappa coefficients. Kappa ranges strength of agreement were interpreted as follows: <0.00 poor; 0.00-0.2 slight; 0.21-0.4 fair; 0.41-0.6 moderate; 0.61-0.8 substantial; 0.81-1 almost perfect. The percent of agreement was displayed as well. All confidence intervals were based on normal approximation with a significance level of 0.05.

The data were analysed using SAS[®] version 9.3 (SAS Institute, Cary North Carolina). Confidence intervals for null proportions were computed with R version 3.1.2. (R Foundation for Statistical Computing, Vienna, Austria).

Results

Twenty patients (9 females and 11 males) with chronic rhinosinusitis (Lund-Mackay score range (6-24) were included in the study.

According to the rhinologist's observations, CT was superior to

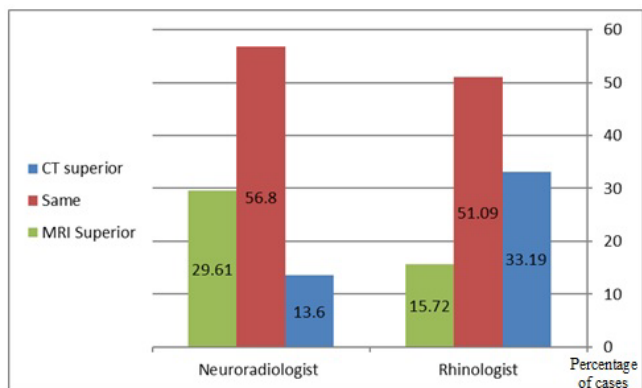


Figure 1. Distribution of MRI vs. CT comparison grades by specialist.

MRI in 33.2% of cases (95% CI, 28.9%-37.5%), CT was same as MRI in 51.1% (95% CI, 46.5%-55.7%), and MRI was superior to CT in 15.7% (95% CI, 12.4%-19.1%). Overall, MRI was found to be the same as CT or superior to it in 66.8% of cases (95% CI, 62.5%-71.1%).

According to the neuroradiologist’s observations, CT was superior to MRI in 13.6% of cases (95% CI, 10.5%-16.7%), CT was same as MRI in 56.8% (95% CI, 52.3%-61.3%) and MRI was superior to CT in 29.6% of cases (95% CI, 25.4%-33.8%). Overall, MRI was found to be the same as CT or superior to it in 86.4% of cases (95% CI, 83.3%-89.6%).

Both the rhinologist and neuroradiologist did not report any image comparisons that were grade 1, i.e., “not visible on MRI” (Figure 1).

The anatomical structures were divided into 3 groups according to the rhinologist’s evaluation of their visibility on MRI images as compared to CT. The following anatomic details visualized on MRI were deemed by the rhinologist as the same, or better than CT in >75% of patients (Table 2): inferior turbinates (n=19, 95%), maxillary sinus (n=19, 95%), Agger nasi (n=18, 90%), middle turbinates (n=18, 90%), posterior ethmoid artery canal (n=18, 90%), sphenoid septae (n=17, 85%), septum (n=16, 80%) and anterior ethmoid artery canal (n=16, 80%). Representative examples are shown in Figure 3A-E.

As shown in Table 3, according to the rhinologist, MRI was superior to, or the same as CT in 50-75% of patients when visualizing the bulla (n=15, 75%), sphenoid sinus (n=15, 75%), uncinata process (n=15, 75%), frontal septae (n=15, 75%), frontal sinus (n=13, 65%), lamina papyracea (n=13, 65%), sella turcica (n=12, 60%), vidian canal (n=11, 55%) and carotid artery canal (n=11, 55%). An example case demonstrating a lamina papyracea defect on MRI compared with CT is illustrated in Figure 3F.

As shown in Table 4, the following anatomic details visualized on MRI were deemed by the rhinologist as the same, or better than, CT in ≤50% of patients: the optic nerve canal (n=10, 50%), superior turbinates (n=9, 45%), ethmoid septae (n=9, 45%), rotundum canal (n=8, 40%), cribriform plate (n=6, 30%) and infra orbital nerve canal (n=5, 25%).

Kappa analysis to evaluate the magnitude of agreement between the evaluations of the rhinologist and the neuroradiologist showed that overall agreement was 77.6% (Kappa =0.41; Table 5).

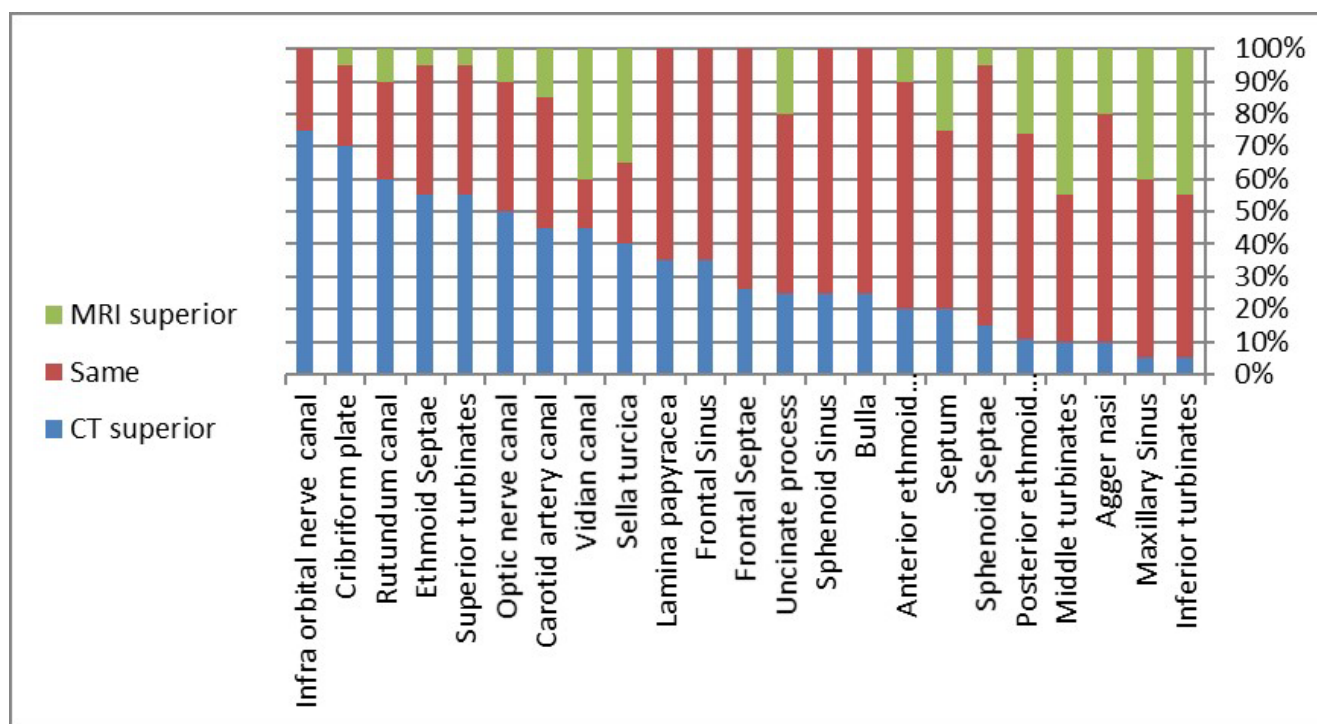


Figure 2. Distribution of MRI vs. CT comparison grade by anatomical structures – rhinologist evaluation.

Table 2. Anatomical structures observed on MRI and graded by the rhinologist as superior to, or the same as CT in >75% of cases.

Anatomic structure	Comparison grade	Patients N=20 n (%)	95% Confidence interval
Inferior turbinates	CT Superior to MRI	1 (5)	0.00-14.55
	Same	10 (50)	28.09-71.91
	MRI superior to CT	9 (45)	23.20-66.80
	CT Superior to MRI	1 (5)	0.00-14.55
	Same	11 (55)	33.20-76.80
	MRI superior to CT	8 (40)	18.53-61.47
	CT Superior to MRI	2 (10)	0.00-23.15
	Same	14 (70)	49.92-90.08
	Maxillary sinus	4 (20)	2.47-37.53
Middle turbinates		2 (10)	0.00-23.15
		9 (45)	23.20-66.80
Agger nasi		9 (45)	23.20-66.80
	CT Superior to MRI	2 (10)	0.00-24.33
	Same	13 (65)	41.47-84.85
Posterior ethmoid artery canal		5 (25)	6.02-43.98
	CT Superior to MRI	3 (15)	0.00-30.65
	Same	16 (80)	62.47-97.53
Sphenoid septae		1 (5)	0.00-14.55
	CT Superior to MRI	4 (20)	2.47-37.53
	Same	11 (55)	33.20-76.80
Septum		5 (25)	6.02-43.98
	CT Superior to MRI	4 (20)	2.47-37.53
	Same	14 (70)	49.92-90.08
Anterior ethmoid artery canal		2 (10)	0.00-23.15
	CT Superior to MRI	4 (20)	2.47-37.53
	Same	14 (70)	49.92-90.08
	MRI superior to CT	2 (10)	0.00-23.15

Discussion

CT is currently regarded as a mandatory scan prior to, and during ESS⁽⁹⁻¹¹⁾. CT is considered better at demonstrating bony structures and remains the gold standard for imaging sinus pathology, while MRI is usually used as a complementary scan only in selected cases. In a study by Hähnel et al.⁽¹²⁾, CT and MRI of patients with inflammatory paranasal sinus disease were evaluated subjectively by two neuroradiologists (without rhinologist) and confirmed the common opinion that CT is superior to MRI for planning ESS.

The advancement of CT imaging has led to reduced long-term cancer risk following the use of this technology^(1, 13). Nonetheless, there is direct evidence from epidemiologic studies that the ionizing radiation doses delivered by some CT scanners are in ranges linked to increased risk of cataract and malignant tumour development. This evidence is convincing and applies to both adults and children⁽²⁻⁶⁾. Cone Beam Computed Tomo-

Table 3. Anatomical structures observed on MRI and graded by the rhinologist as superior to, or the same as CT in 50-75% of cases.

Anatomic structure	Comparison grade	Patients N=20 n (%)	95% Confidence interval
Bulla	CT superior to MRI	5 (25)	6.02-43.98
	Same	15 (75)	56.02-93.98
	MRI superior to CT	0 (0)	
Sphenoid sinus	CT superior to MRI	5 (25)	6.02-43.98
	Same	15 (75)	56.02-93.98
	MRI superior to CT	0 (0)	
Uncinate process	CT superior to MRI	5 (25)	6.02-43.98
	Same	11 (55)	33.20-76.80
	MRI superior to CT	4 (20)	2.47-37.53
Frontal septae	CT superior to MRI	5 (25)	6.02-43.98
	Same	15 (75)	56.02-93.98
	MRI superior to CT	0 (0)	
Frontal sinus	CT superior to MRI	7 (35)	14.10-55.90
	Same	13 (65)	44.10-85.90
	MRI superior to CT	0 (0)	
Lamina papyracea	CT superior to MRI	7 (35)	14.10-55.90
	Same	13 (65)	44.10-85.90
	MRI superior to CT	0 (0)	
Sella turcica	CT superior to MRI	8 (40)	18.53-61.47
	Same	5 (25)	6.02-43.98
	MRI superior to CT	7 (35)	14.10-55.90
Vidian canal	CT superior to MRI	9 (45)	23.20-66.80
	Same	3 (15)	0.00-30.65
	MRI superior to CT	8 (40)	18.53-61.47
Carotid artery canal	CT superior to MRI	9 (45)	23.20-66.80
	Same	8 (40)	18.53-61.47
	MRI superior to CT	3 (15)	0.00-30.65

graphy (CBCT), a low-dose volumetric imaging technique, is a good alternative to conventional CT as an imaging technique of bony structures in children as well as in adults^(7, 14, 15). CBCT of the paranasal sinuses delivers the same radiation dosage as an X-ray examination of the chest⁽¹⁶⁻¹⁸⁾. According to Lechuga et al.⁽¹⁹⁾, chronic sinusitis is an emerging indication for CBCT in the anterior skull region; however, conventional CT shows superior soft tissue differentiation with apparently more uniform, accurate and clear images⁽²⁰⁾.

Compared with a CT scan, MRI has a known high sensitivity for demonstrating inflammatory processes, malignant tissue, brain and orbital structures⁽²¹⁻²⁴⁾. In the study reported here, our novel MRI protocol was shown to be equal, or superior to CT for assessing paranasal anatomy in 66.8% and 86.4% of structures

Table 4. Anatomical structures observed on MRI and graded by the rhinologist as superior to, or the same as CT in <50% of cases.

Anatomic structure	Comparison grade	Patients N=20 n (%)	95% Confidence interval
Optic nerve canal	CT superior to MRI	10 (50)	28.09-71.91
	Same	8 (40)	18.53-61.47
	MRI superior to CT	2 (10)	0.00-23.15
Superior turbinates	CT superior to MRI	11 (55)	33.20-76.80
	Same	8 (40)	18.53-61.47
	MRI superior to CT	1 (5)	0.00-14.55
Ethmoid septae	CT superior to MRI	11 (55)	33.20-76.80
	Same	8 (40)	18.53-61.47
	MRI superior to CT	1 (5)	0.00-14.55
Rotundum canal	CT superior to MRI	12 (60)	38.53-81.47
	Same	6 (30)	9.92-50.08
	MRI superior to CT	2 (10)	0.00-23.15
Cribriform plate	CT superior to MRI	14 (70)	49.92-90.08
	Same	5 (25)	6.02-43.98
	MRI superior to CT	1 (5)	0.00-14.55
Infra orbital nerve canal	CT superior to MRI	15 (75)	56.02-93.98
	Same	5 (25)	6.02-43.98
	MRI superior to CT	0 (0)	

evaluated by a rhinologist and neuroradiologist, respectively. Although analysis by organs showed similar results, they should be treated with caution due to the limited sample size. The evaluation of MRI and CT images may have been influenced by the greater experience of the neuroradiologist in interpreting MRI images, while the rhinologist, due to routine usage of CT scans during surgery, has an advantage in interpreting CT images. It may be assumed that with time and training, the interpretation of MRI by the rhinologist will improve, increasing the percent of similarity between the rhinologist and neuroradiologist. In addition, as an experienced rhinologist does not necessarily need information about subtle anatomical variations, an adequate imaging of the anatomy combined with an advantage in demonstrating soft tissues may sometimes be preferable. Our findings suggest that for certain anatomical structures MRI is superior to CT and can be a powerful tool for assessing anterior and posterior ethmoidal arteries, vidian and carotid artery canal, frontal and sphenoid sinuses, and septae, inferior and middle turbinates, lamina papyracea, agger nasi, bulla, uncinate process, maxillary sinus, nasal septum and sella turcica. MRI manufacturers are aware of noise exposure and claustrophobia issues involved with the use of this technology, and over the years they have modified MRI designs to help ease patient

Table 5. Agreement between the rhinologist and neuroradiologist.

Anatomical structure	MRI 'superior' or 'same' vs. CT 'superior' between the rhinologist and neuroradiologist	
	Kappa	Percent of agreement
All	0.41	77.63
Middle turbinates	1	100
Inferior turbinates	NA	95
Maxillary sinus	NA	95
Agger nasi	NA	90
Sella turcica	0.78	90
Posterior ethmoid artery canal	0.44	89.47
Sphenoid septae	NA	85
Uncinate process	0.5	85
Lamina papyracea	0.63	85
Vidian canal	0.68	84.21
Septum	NA	80
Superior turbinates	0.6	80
Bulla	0.27	80
Sphenoid Sinus	0.27	78.95
Frontal Sinus	0.34	75
Anterior ethmoid artery canal	-0.09	75
Carotid artery canal	0.48	75
Rotundum canal	0.53	75
Frontal septae	NA	73.68
Optic nerve canal	0.33	65
Ethmoid septae	0.08	50
Infra orbital nerve canal	0.11	40
Cribriform plate	0.09	40

anxiety^(25,26). However, when considering to use MRI, some other disadvantages must be taken into account, including the need for insurance preauthorization due to increased costs, lower availability and longer examination time. Yet, in cases in which the use of CT scans prior to ESS appears questionable, and given the complete absence of ionizing radiation, MRI enables the assessment of radiosensitive populations such as children, pregnant women, and patients with repeated exposure to radiation. The risks of using gadolinium-based contrast agents (GBCA) should also be addressed due to their popular use in diagnostic imaging. Intravenous administration of GBCA is associated with contrast deposition in neuronal tissues that is unrelated to renal or hepatobiliary dysfunction^(27,28). Despite uncertainties and while additional studies are needed, it seems reasonable to recommend using GBCA only when clinically necessary and at

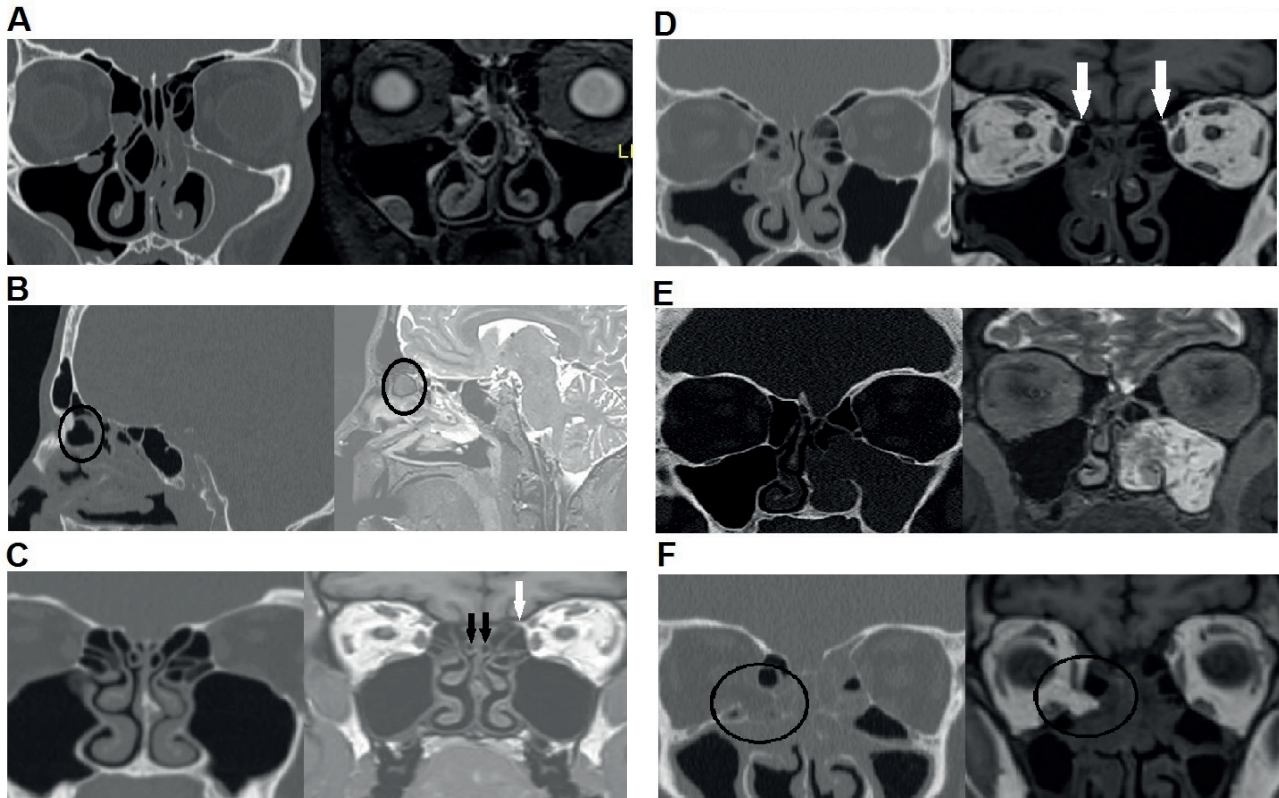


Figure 3. Representative images of anatomical structures on MRI and CT. (A) The large concha bullosa of the right nasal cavity and the middle turbinate of the left nasal cavity, as well as the inferior turbinates and the maxillary sinuses are well demonstrated on CT (left image) and T2-weighted MRI images (right image). (B) Agger nasi cells (black circle) and the frontal, ethmoid and sphenoid sinuses are well demonstrated on a T2-weighted MRI image. (C) The ethmoid septae are clearly seen in the T1-weighted MRI image. The middle and inferior turbinates are well demonstrated. The aerated superior turbinates are marked by the black arrows. The course of the left anterior ethmoid artery is marked by the white arrow. (D) The anterior ethmoid arteries (white arrows) are well demonstrated by T1-weighted MRI. The contour of the lamina papyracea is very clear. As expected, the contents of the orbit can be seen more clearly on the MRI image compared to the CT image. (E) Both CT and MRI images clearly demonstrate an antro-nasal mass, but only the MRI image clearly shows the typical cerebriform pattern of inverted papilloma. (F) This CT image might be interpreted as severe ethmoid mucosal disease, but the MRI image clearly shows the fat herniating from the orbit (black circles). (G) Although the cribriform plate and lateral lamellae (black circles) are generally sharper on a CT image, they can also be clearly seen on an MRI image.

the lowest possible dose. In the current study the MRI protocol was unenhanced.

Our study is not without limitations. As each structure was first identified on the CT scan, then on MRI, this type of experimental setup may favour one of the modalities over the other. Clinical experience is important in translating images to expected operative findings. For this reason, a study measuring and comparing the data from more than one rhinologist would be an advantage. In addition, we acknowledge that the practicality of using MRI for preoperative and intraoperative assessment by most sinus surgeons is a concern. Although it is easy to adjust the contrast of MRI images to highlight the patient's anatomy, the routine sinus surgeon would have difficulties making such adjustments without appropriate training and education. CT imaging is still the workhorse tool used for ESS. Given its advantages, MRI should be considered as an option in selected cases.

Conclusion

The rhinologist prefers CT demonstration of bony structures, while the neuroradiologist prefers MRI. Still, with the MRI protocol used in this study, according to both, most bony structures are well demonstrated by MRI. It is suggested that if supported by additional studies, in certain and highly selected indications, the surgeon would be able to rely on MRI preoperatively and during surgery. Consequently, the surgeon will be able to clearly visualize both hard and soft tissue features while reducing patients' exposure to radiation.

Authorship contribution

RL and SS (equal contribution): Study design, data collection, data evaluation and manuscript writing. JL: Study design, data collection, data evaluation and manuscript writing. MM, AM and MG: Data collection and evaluation.

Acknowledgments

None.

Funding

None.

Ethics approval and consent to participate

No approval or consent needed.

Consent for publication

Not applicable.

Availability of data and materials

Not applicable.

Conflict of interest

The authors have no conflicts of interest to disclose.

References

- Bassim MK, Ebert CS, Sit RC, Senior BA. Radiation dose to the eyes and parotids during CT of the sinuses. *Otolaryngol Head Neck Surg.* 2005; 133: 531-533.
- Brenner DJ, Hall EJ. Computed tomography—an increasing source of radiation exposure. *N Engl J Med.* 2007; 357: 2277-2284.
- Brenner D, Elliston C, Hall E, Berdon W. Estimated risks of radiation-induced fatal cancer from pediatric CT. *AJR Am J Roentgenol.* 2001; 176: 289-296.
- Chodick G, Ronckers CM, Shalev V, Ron E. Excess lifetime cancer mortality risk attributable to radiation exposure from computed tomography examinations in children. *Isr Med Assoc J.* 2007; 9: 584-587.
- Pearce MS, Salotti JA, Little MP, et al. Radiation exposure from CT scans in childhood and subsequent risk of leukaemia and brain tumours: a retrospective cohort study. *Lancet.* 2012; 380: 499-505.
- Preston DL, Ron E, Tokuoka S, et al. Solid cancer incidence in atomic bomb survivors: 1958-1998. *Radiat Res.* 2007; 168: 1-64.
- Dammann F. Imaging of paranasal sinuses today. *Radiologe.* 2007; 47: 576, 578-583.
- Swartz JD, Russell KB, Wolfson RJ, Marlowe FI. High resolution computed tomography in evaluation of the temporal bone. *Head Neck Surg.* 1984; 6: 921-931.
- Stammlerberger H. Endoscopic endonasal surgery – new concepts in treatment of recurring sinusitis. II. Surgical technique. *Otolaryngol Head Neck Surg.* 1985; 94: 147-156.
- Lund, VJ, Savvy, L, Lloyd, G. Imaging for endoscopic sinus surgery in adults. *J Laryngol Otol.* 2000; 114: 395-397.
- Duvoisin B, Landry M, Chapuis L, Krayenbuhl M, Schnyder P. Low-dose CT and inflammatory disease of the paranasal sinuses. *Neuroradiology.* 1991; 33: 403-406.
- Hähnel S, Ertl-Wagner B, Tasman AJ, Forsting M, Jansen O. Relative value of MR imaging as compared with CT in the diagnosis of inflammatory paranasal sinus disease. *Radiology.* 1999; 210: 171-176.
- McCollough CH, Bushberg JT, Fletcher JG, Eckel LJ. Answers to common questions about the use and safety of CT scans. *Mayo Clin Proc.* 2015; 90: 1380-1392.
- Nardi C, Salerno S, Molteni R, et al. Radiation dose in non-dental cone beam CT applications: a systematic review. *Radiol Med.* 2018; 123: 765-777.
- Stutzki M, Jahns E, Mandapathil MM, Diogo I, Werner JA, Güldner C. Indications of cone beam CT in head and neck imaging. *Acta Otolaryngol.* 2015; 135: 1337-1343.
- Güldner C, Ningo A, Voigt J, et al. Potential of dosage reduction in cone-beam-computed tomography (CBCT) for radiological diagnostics of the paranasal sinuses. *Eur Arch Otorhinolaryngol.* 2013; 270: 1307-1315.
- Lell MM, May MS, Brand M, et al. Imaging the paranasal region with a third-generation dual-source CT and the effect of tin filtration on image quality and radiation dose. *AJNR Am J Neuroradiol.* 2015; 36: 1225-1230.
- Walliczek-Dworschak U, Diogo I, Strack L, Mandapathil M, Teymoortash A, Werner JA, Güldner C. Indications of cone beam CT in head and neck imaging in children. *Acta Otorhinolaryngol Ital.* 2017; 37: 270-275.
- Lechuga L, Weidlich GA. Cone beam CT vs. fan beam CT: A comparison of image quality and dose delivered between two differing CT imaging modalities. *Cureus.* 2016; 8(9): e778.
- Leiva-Salinas C, Flors L, Gras P, et al. Dental flat panel conebeam CT in the evaluation of patients with inflammatory sinonasal disease: Diagnostic efficacy and radiation dose savings. *AJNR Am J Neuroradiol.* 2014; 35: 2052-2057.
- Som PM, Shapiro MD, Biller HF, Sasaki C, Lawson W. Sinonasal tumors and inflammatory tissues: differentiation with MR imaging. *Radiology.* 1988; 167: 803-808.
- Som PM, Shugar JM, Troy KM, Sacher M, Stollman AL. The use of magnetic resonance and computed tomography in the management of a patient with intrasinus hemorrhage. *Arch Otolaryngol Head Neck Surg.* 1988; 114: 200-202.
- Zinreich SJ, Kennedy DW, Malat J, et al. Fungal sinusitis: Diagnosis with CT and MR imaging. *Radiology.* 1988; 169: 439-444.
- Lloyd GA, Lund VJ, Phelps PD, Howard DJ. Magnetic resonance imaging in the evaluation of nose and paranasal sinus disease. *Br J Radiol.* 1987; 60: 957-968.
- Bangard C, Paszek J, Berg F, Eyl G, Kessler J, Lackner K, Gossmann A. MR imaging of claustrophobic patients in an open 1.0T scanner: motion artifacts and patient acceptability compared with closed bore magnets. *Eur J Radiol.* 2007; 64: 152-157.
- Dewey M, Schink T, Dewey CF. Claustrophobia during magnetic resonance imaging: cohort study in over 55,000 patients. *J Magn Reson Imaging.* 2007; 26: 1322-1327.
- Ramalho J, Ramalho M. Gadolinium Deposition and Chronic Toxicity. *Magn Reson Imaging Clin N Am.* 2017; 25: 765-778.
- McDonald RJ, McDonald JS, Kallmes DF, et al. Intracranial gadolinium deposition after contrast-enhanced MR imaging. *Radiology.* 2015; 275: 772-782.

Dr. Shay Schneider
A.R.M. Center of Otolaryngology
Head and Neck Surgery
Assuta Medical Centers
20 Habarzel Street
Tel Aviv
Israel

Tel: +972-3-7645464,
+972-54-7685189.

E-mail: shayfroind48@gmail.com,
shayfr@clalit.org.il